

# KOPIO TN139draft

## Background from some non- $K_L^0$ sources

David E. Jaffe, BNL

August 5, 2005

### Abstract

Backgrounds due to stopped muons in coincidence with the products of the  $K_L^0$  decay and backgrounds due to non- $K_L^0$  sources upstream of the decay region are estimated to be negligible with the FastMC.

## 1 Introduction

This note deals primarily with the estimated rates of two potential backgrounds using the FastMC:

1. Background due to the accidental coincidence of a  $K_L^0$  decay and the products of a stopped muon decay. This background is denoted by the acronym **stpm**.
2. Background due to non- $K_L^0$  sources that produce photons that emanate from upstream of the decay region. This background is denoted by the acronym **nonkl**.

Distributions of backgrounds previously discussed and presented in TN137 [1] are also shown for comparison purposes. Background from  $K_L^0 \rightarrow \pi^0\pi^0\pi^0$  ( $K_L^0 \rightarrow \pi^0\pi^0$ ) decays upstream of the decay regions are denoted by **kp3.us(kp2.us)**. Background from pairs of  $K_L^0$  decays upstream of the decay region are denoted by **all2.us**. Signal decays in the decay region are denoted by **kpnn**.

**This note deals only with the  $2\gamma$ PR detection method.** If units are omitted from a figure or text, assume centimeters, nanoseconds, or MeV as appropriate. The detector geometry, notation and terms in this note are the same as TN137 [1].

## 2 Simulation of stopped muons

The background due to the accidental coincidence of a  $K_L^0$  decay and the products of a stopped muon decay is estimated by generating a single  $K_L^0$  decay from  $z = 47$  to 1397 cm (from the spoiler to the downstream end of the decay region). The  $K_L^0$  are allowed to decay freely according to the known branching fractions. The products of stopped, decaying muons are added to each event according to the description in the FastMC user manual [2]. Briefly, the muon decay position, electron energy and direction are interpreted as the photon conversion point, energy and direction and the standard smearing in position, energy and angle in the PR is performed. The rate of stopped muons is taken from a GEANT3 simulation that assumed that 3.57 is the mean number of  $K_L^0$  exiting the spoiler per microbunch.

Only  $\pi^0$  candidates that contained at least one photon candidate from a stopped muon were accepted for further analysis. In addition the same loose 'skim' cuts as in TN137 [1] were applied. A total of  $3.1 \times 10^9$  events were generated and 7286836 (0.235%) events satisfied the 'skim' cuts with the requirement of at least one photon candidate from a stopped muon.

### 3 Simulation of non- $K_L^0$ background

The background due to non- $K_L^0$  sources was estimated using a sample of events generated by Andrei Poblagev using a GEANT3 simulation of the spoiler and collimator system. For all particles with more than 10 MeV of kinetic energy that reach  $z = 850$  cm (the downstream end of D3), the event number, particle species, position, time and three-momentum are recorded. Particles are drawn from this list based on the expected number of protons per microbunch incident upon the primary target (taken to be  $1 \times 10^6$  following the assumptions in TN138 [3]). Correlations between the particles are correctly taken into account by selecting all particles produced by a single incident proton. The original generated list corresponded to  $1 \times 10^{12}$  incident protons.

To attempt to improve the statistical impact, an event-mixing technique was applied. The original list was duplicated and the entries corresponding to the first 12 incident protons were removed. Particles were then selected sequentially from each of the two lists assuming  $0.5 \times 10^6$  protons/microbunch for each list. The FastMC was run in jobs of  $1 \times 10^7$  events per job and the entry number of the last particle selected from each list in a job was used as the starting point in each list for the subsequent job.

Despite this attempt to randomize the selection, the resulting candidates are still dominated by photons produced by a few original incident protons. Evidence of this can be seen in the distributions of kinematic quantities from the **nonkl** candidates. The fraction of  $\pi^0$  candidates passing the “GeomAcc” and “GoodFit” cuts that result from a two different incident protons is only  $\sim 0.2\%$ . An improved sample of particles is needed to obtain a more reliable estimate of the **nonkl** background. Apart from a computationally intensive approach to augment the statistics of the sample by a significant factor ( $\sim 100$ ), no solution is readily available; at least, Andrei and I could not think of one. The generation of the original sample took approximately 1 week of CPU time on a single processor.

A total of  $2.01 \times 10^9$  FastMC events were generated and 14842072 (0.738%) events satisfied the ‘skim’ cuts.

### 4 Discussions of distributions

I remind the reader that the cut names are defined and described in Section 3 of TN137 [1].

In general the distributions reflect the fact that the **kpnn**, **kp3.us**, **kp2.us**, and **nonkl** candidates are due to photons that originate from a single point in space and time, whilst the **stpm** and **all2.us** candidates are due to photons produced at different points in space and/or time. These features are evident in the distribution of **Chi2n** in Figure 1 and in the **deLT** and **XX** distributions in Figures 2 and 3, respectively. For the **XX** distributions in Figure 3, the dominance of a few **nonkl** candidates can be seen.

The **DOCA** distribution for **stpm** in Figure 4 is significantly flatter than the **DOCA** distributions from other sources including **all2.us**. For the backgrounds that originate from upstream of the decay region, the calculated **DOCA** is relatively smaller since the effective source is more localized than for **stpm** candidates.

The sign of the slope of **DK12** distributions (Figure 5) for all backgrounds differs from that of the signal.

In Figure 6, the **kpnn** and **stpm** distributions both peak at low **sgZK1** in contrast to the other backgrounds. Presumably this is due to the fact that for **stpm**, **sgZK1** is dominated by the higher energy photon from  $K_L^0$  decay.

Figure 7 shows the main cut that is designed to suppress the **stpm** background. The cut is made in the plane of the energy of the lower energy photon candidate **Eg** vs **chi2n** and was designed based on an earlier set of selection criteria. Based on the distributions in Figure 7, it appears that better background suppression could be achieved with a tighter cut in **chi2n** at higher energy and that some **kpnn** acceptance could be

recovered with a looser cut at low energy. It should be noted that the “GeomAcc” and “GoodFit” cuts suppress a great deal of the **stpm** background with low energy photons from the stopped muon. The measured energy of the remaining candidate photons is above the 53 MeV limit for Michel electrons because of the energy resolution. It should be noted that the model for energy smearing is based on simulations at photon energies of 150, 250 and 350 MeV and may not be completely reliable at low energy and for a single  $e^\pm$ .

Figure 8 shows the **Mgg** distributions. The **stpm** and **nonkl** backgrounds are at low mass and only the tails of the distributions contributes to **kpnn** candidates.

The  $T^{*2}$  vs  $\ln(E_{\text{miss}})$  distributions are shown in Figure 9. After the “GeomAcc” and “GoodFit” cuts, the **nonkl** background populates only the low  $T^{*2}$  region that is always excluded by the likelihood cut because it is heavily populated by the background from multibody  $K_L^0$  decays. The **stpm** background occupies more of the plane but seems to be at higher  $\ln(E_{\text{miss}})$  than the signal. The reason for this is not clear.

The distribution of **sgZK1** vs the y-component of the  $K_L^0$  momentum  $p_y(K)$  is shown in Figure 10. The **kpnn** prefers the region near  $\text{sgZK1} = 0$  cm and  $p_y(K) = 0$  MeV/c because of the narrow vertical aperture of the neutral beam line. The **kp3.us**, **kp2.us**, **nonkl** and **all2.us** generally have large **sgZK1**, independent of  $p_y(K)$ ; hence the efficacy of the cut on **sgZK1**. A fraction of the **stpm** background shows a correlation between **sgZK1** and  $p_y(K)$ , perhaps due to the minor influence that the low energy photon has on **sgZK1**.

Figure 11 shows the distribution of  $|y_1 - y_2|$  vs  $|x_1 - x_2|$  where  $y_i$  is the projected  $x$  position of the  $i^{\text{th}}$  candidate photon projected to the  $z$  position of the upstream end of the calorimeter. Signal events cannot populate the region near zero but the backgrounds can. In particular the **nonkl** background has approximately one third of the accepted events near zero that could be excluded without any loss of acceptance.

2005/08/05 10.41

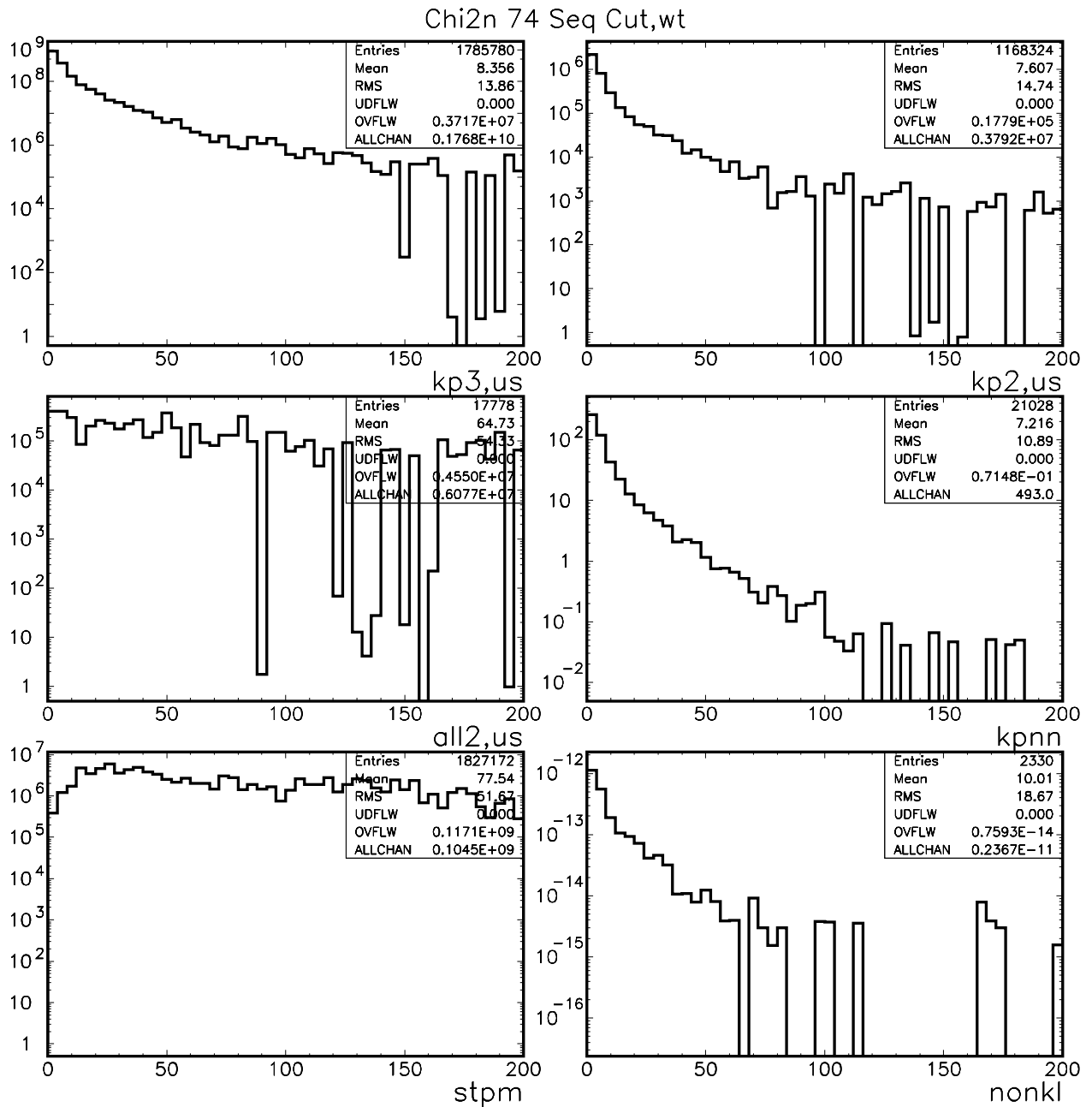


Figure 1: Distribution of Chi2n for  $K_L^0 \rightarrow \pi^0\pi^0\pi^0$ ,  $K_L^0 \rightarrow \pi^0\pi^0$ ,  $2K_L^0$ , signal, stopped muons &  $K_L^0$  and non- $K_L^0$  decays from top, left to right. All cuts prior to the cuts on this distribution are applied. The distributions are weighted.

2005/08/05 10.42

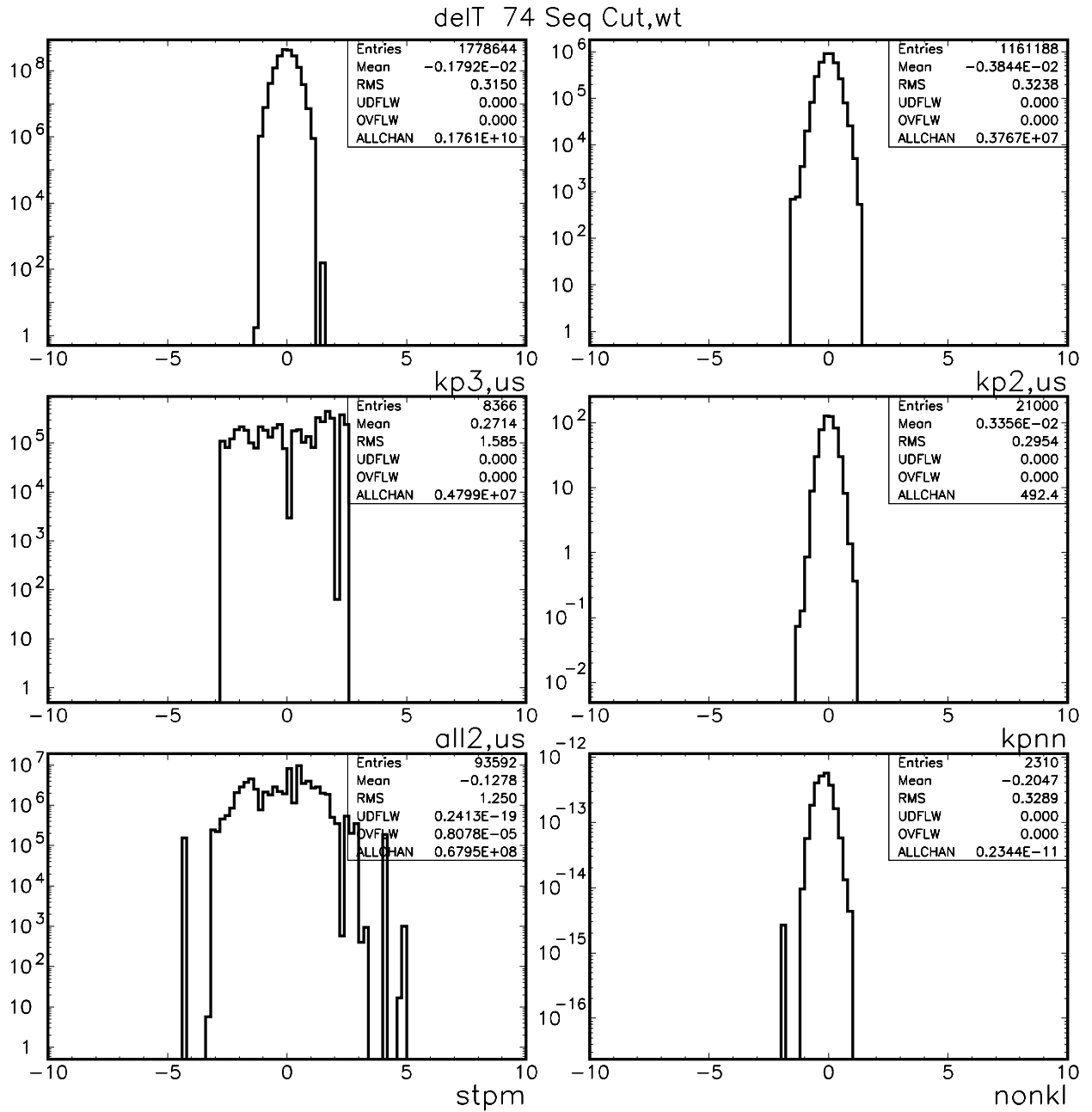


Figure 2: Distribution of  $\delta t$  for  $K_L^0 \rightarrow \pi^0\pi^0\pi^0$ ,  $K_L^0 \rightarrow \pi^0\pi^0$ ,  $2K_L^0$ , signal, stopped muons &  $K_L^0$  and non- $K_L^0$  decays from top, left to right. All cuts prior to the cuts on this distribution are applied. The distributions are weighted.

2005/08/05 10.42

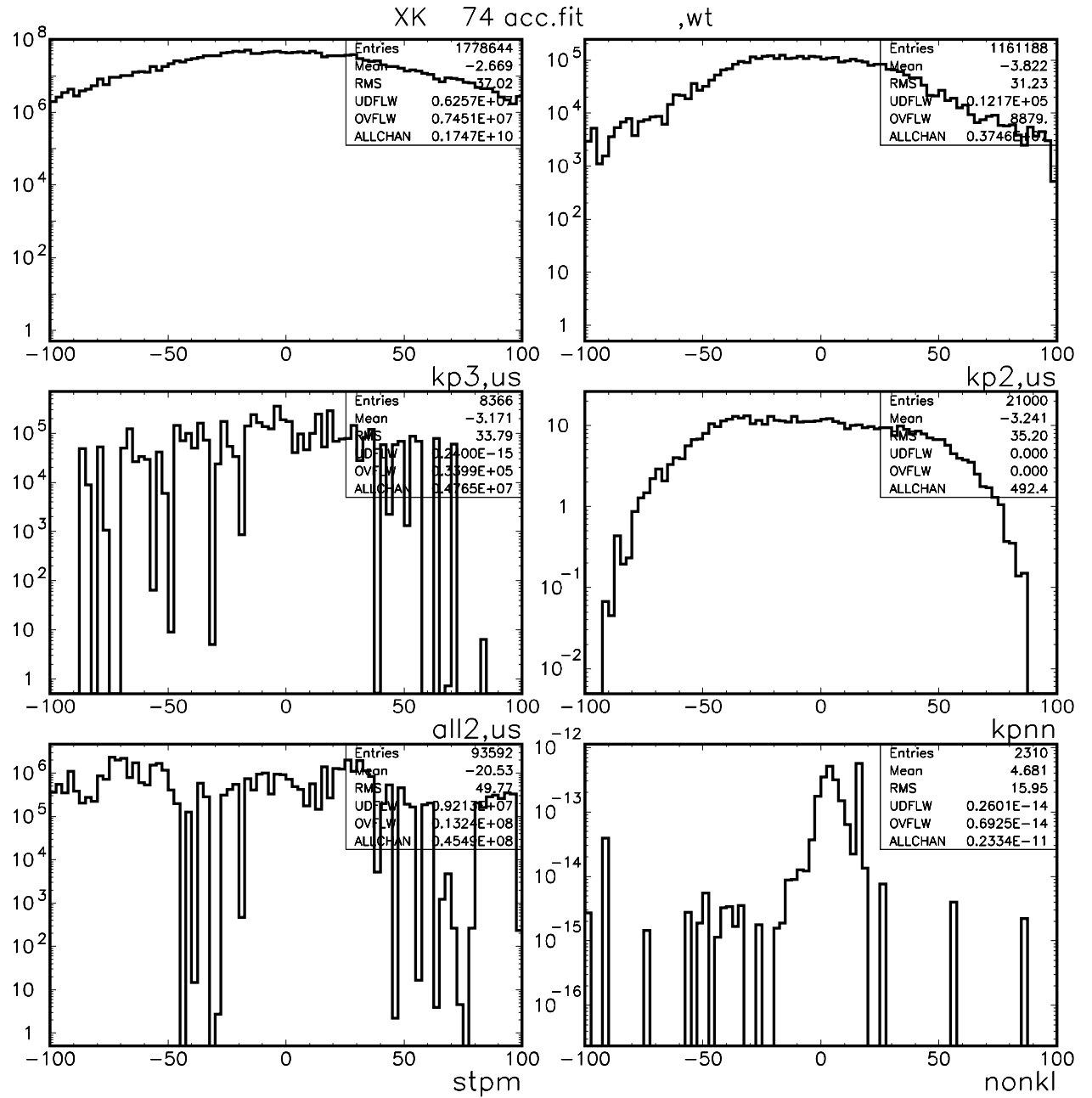


Figure 3: Distribution of XK for  $K_L^0 \rightarrow \pi^0\pi^0\pi^0$ ,  $K_L^0 \rightarrow \pi^0\pi^0$ ,  $2K_L^0$ , signal, stopped muons &  $K_L^0$  and non- $K_L^0$  decays from top, left to right. The “GeomAcc” and “GoodFit” cuts have been applied. The distributions are weighted.

2005/08/05 10.42

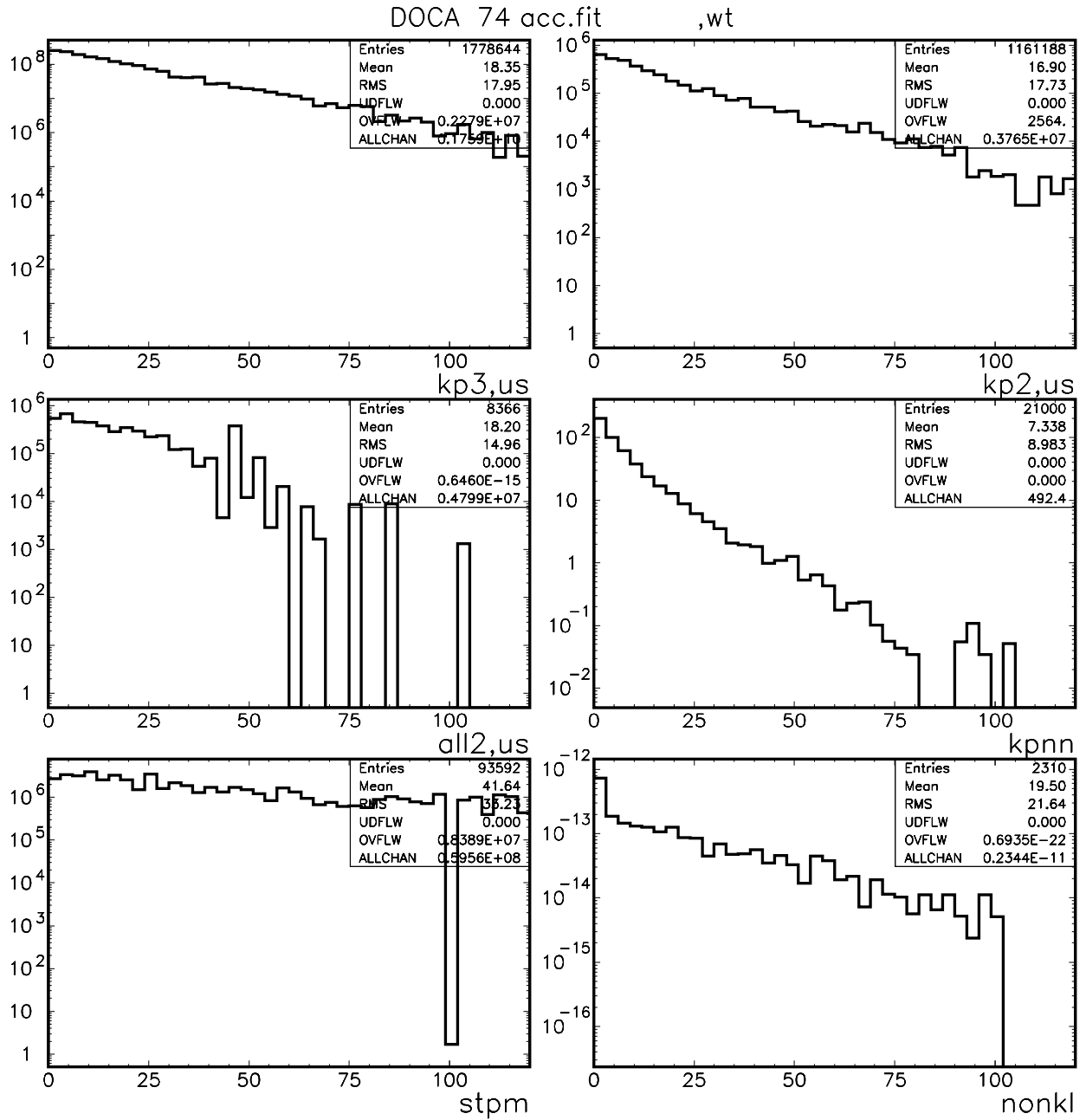


Figure 4: Distribution of DOCA for  $K_L^0 \rightarrow \pi^0\pi^0\pi^0$ ,  $K_L^0 \rightarrow \pi^0\pi^0$ ,  $2K_L^0$ , signal, stopped muons &  $K_L^0$  and non- $K_L^0$  decays from top, left to right. The “GeomAcc” and “GoodFit” cuts have been applied. The distributions are weighted.

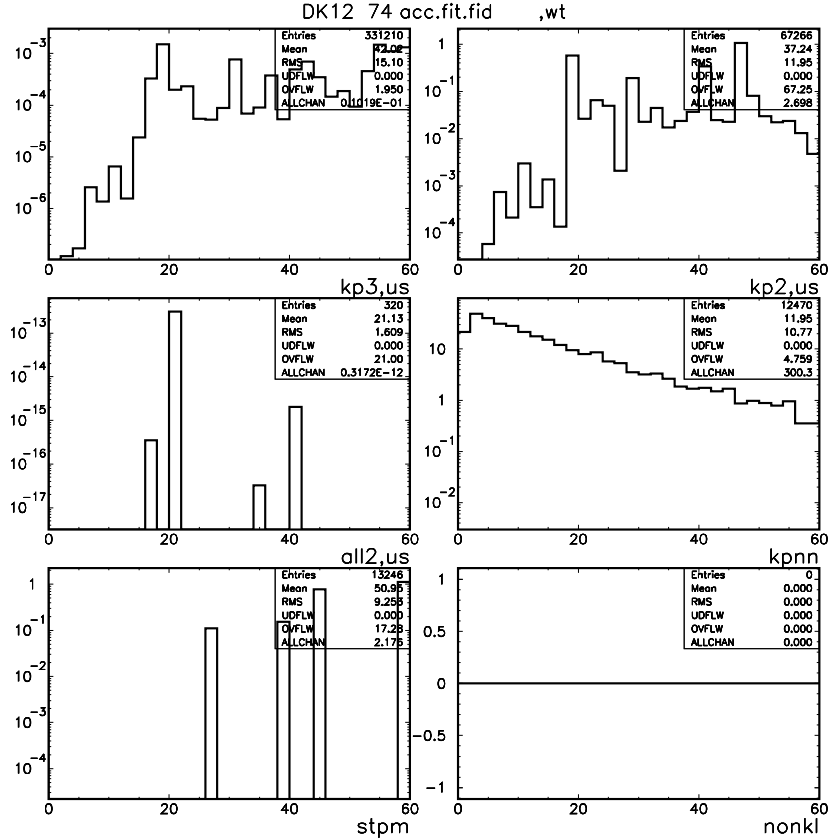
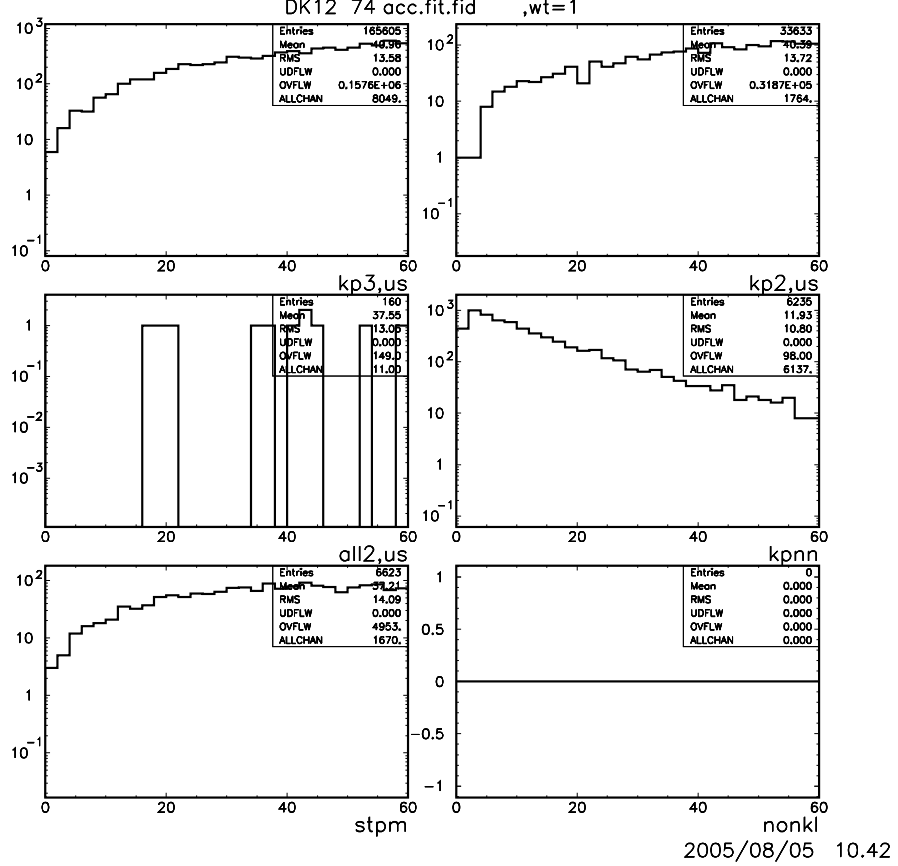


Figure 5: Distribution of DK12 for  $K_L^0 \rightarrow \pi^0\pi^0\pi^0$ ,  $K_L^0 \rightarrow \pi^0\pi^0$ ,  $2K_L^0$ , signal, stopped muons &  $K_L^0$  and non- $K_L^0$  decays from top, left to right. The “GeomAcc” and “GoodFit” cuts have been applied. The top (bottom) six distributions are unweighted(weighted).

2005/08/05 10.42

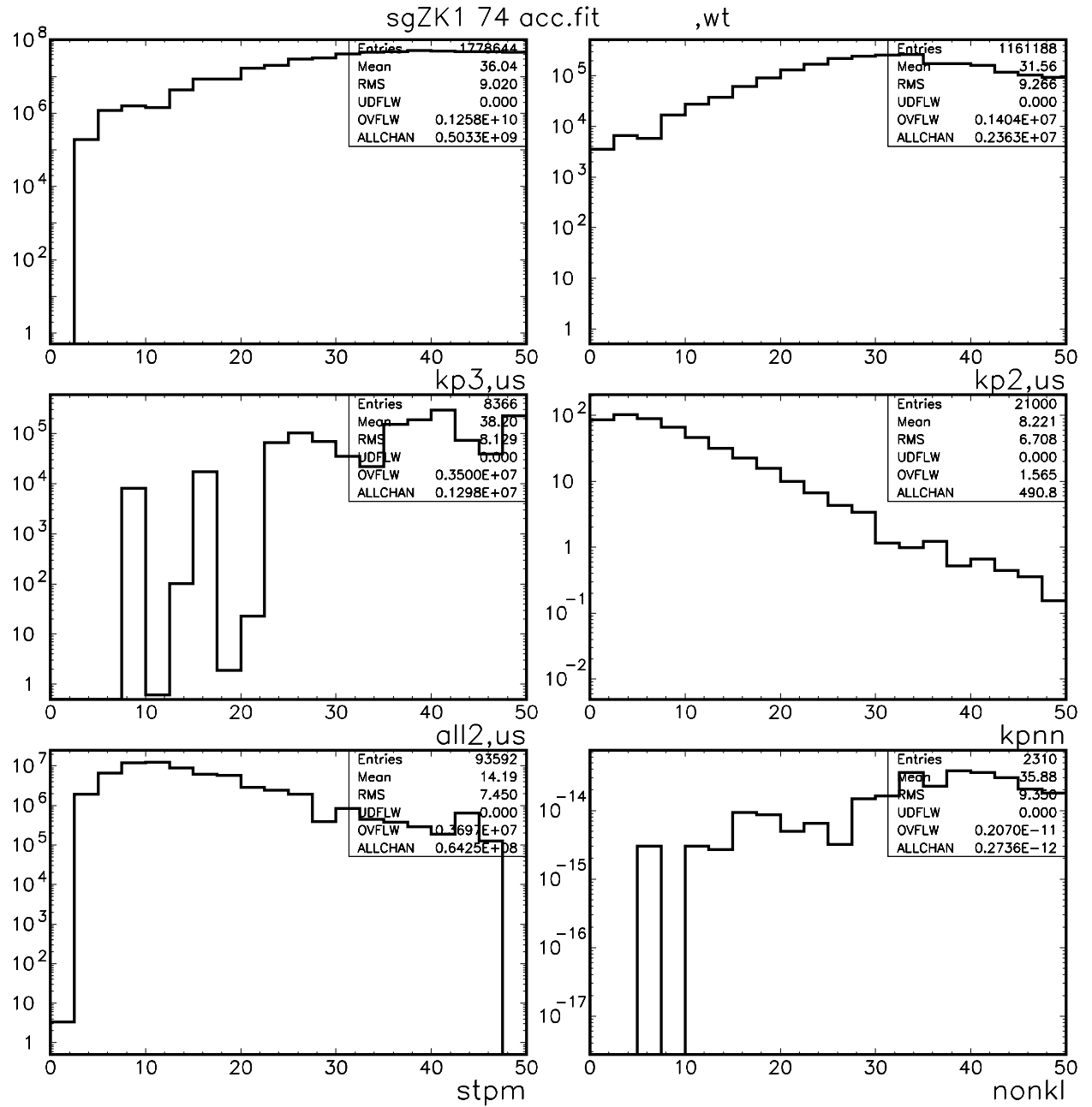


Figure 6: Distribution of sgZK1 for  $K_L^0 \rightarrow \pi^0\pi^0\pi^0$ ,  $K_L^0 \rightarrow \pi^0\pi^0$ ,  $2K_L^0$ , signal, stopped muons &  $K_L^0$  and non- $K_L^0$  decays from top, left to right. The “GeomAcc” and “GoodFit” cuts have been applied. The distributions are weighted.

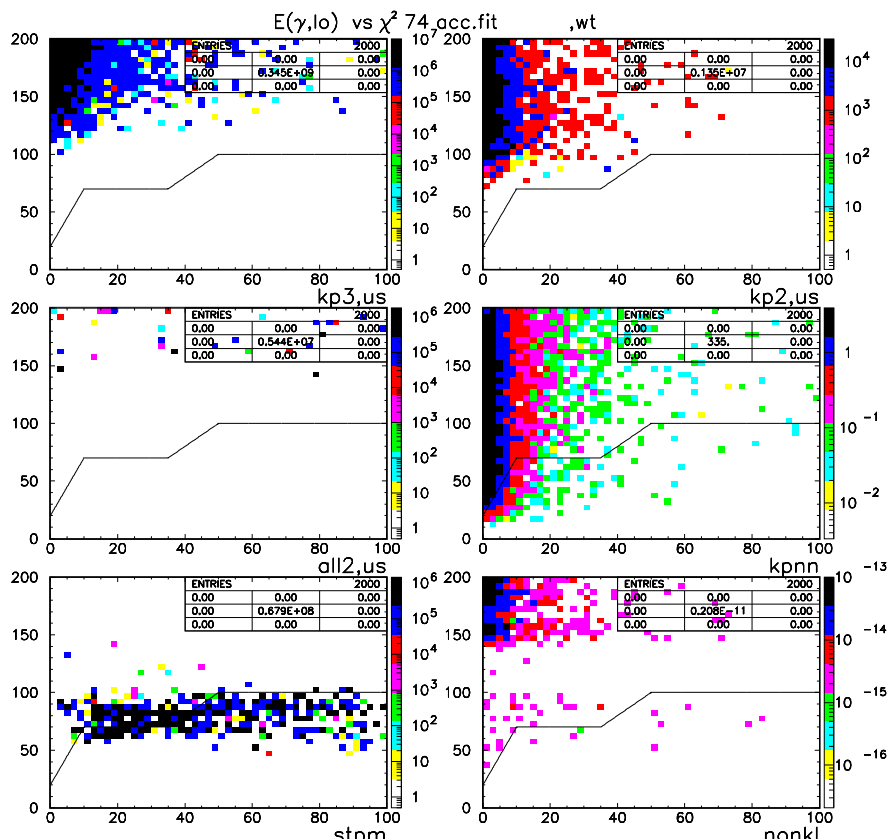
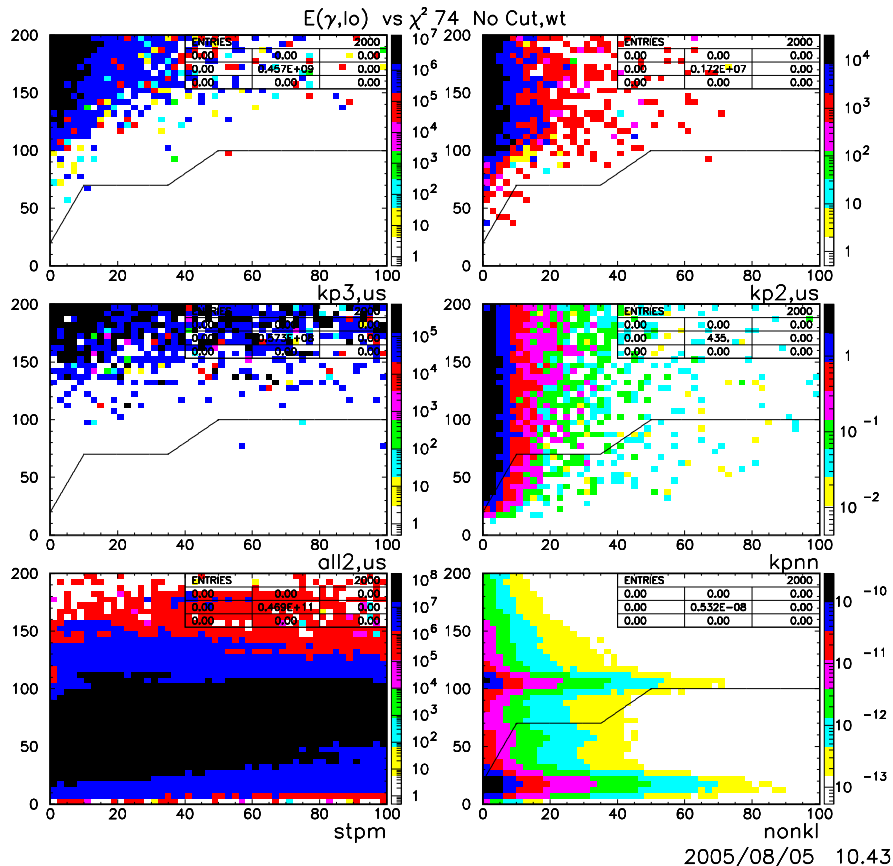


Figure 7: Distribution of the energy of the lower energy photon candidate  $E_{\gamma}$  vs  $\chi^2$  ( $y$  vs  $x$ ) for  $K_L^0 \rightarrow \pi^0 \pi^0 \pi^0$ ,  $K_L^0 \rightarrow \pi^0 \pi^0$ ,  $2K_L^0$ , signal, stopped muons &  $K_L^0$  and non- $K_L^0$  decays from top, left to right. The solid line shows the cut. Candidates above the line are accepted. For the top six distributions, only the 'skim' cuts have been applied. For the bottom six distributions, the 'skim', "GeomAcc" and "GoodFit" cuts have been applied. The distributions are weighted.

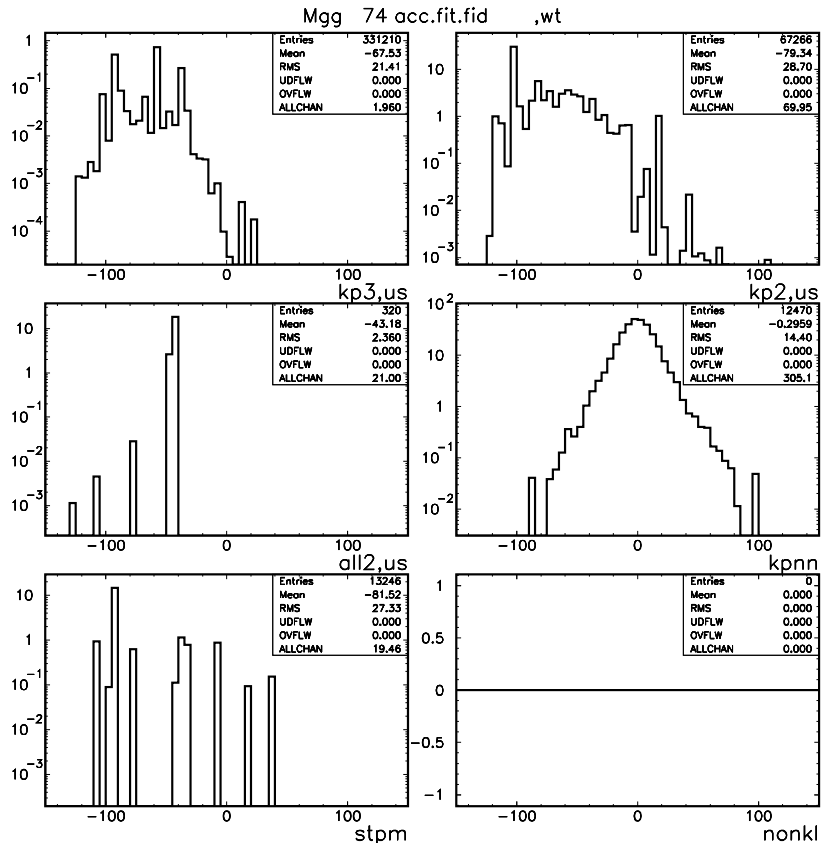
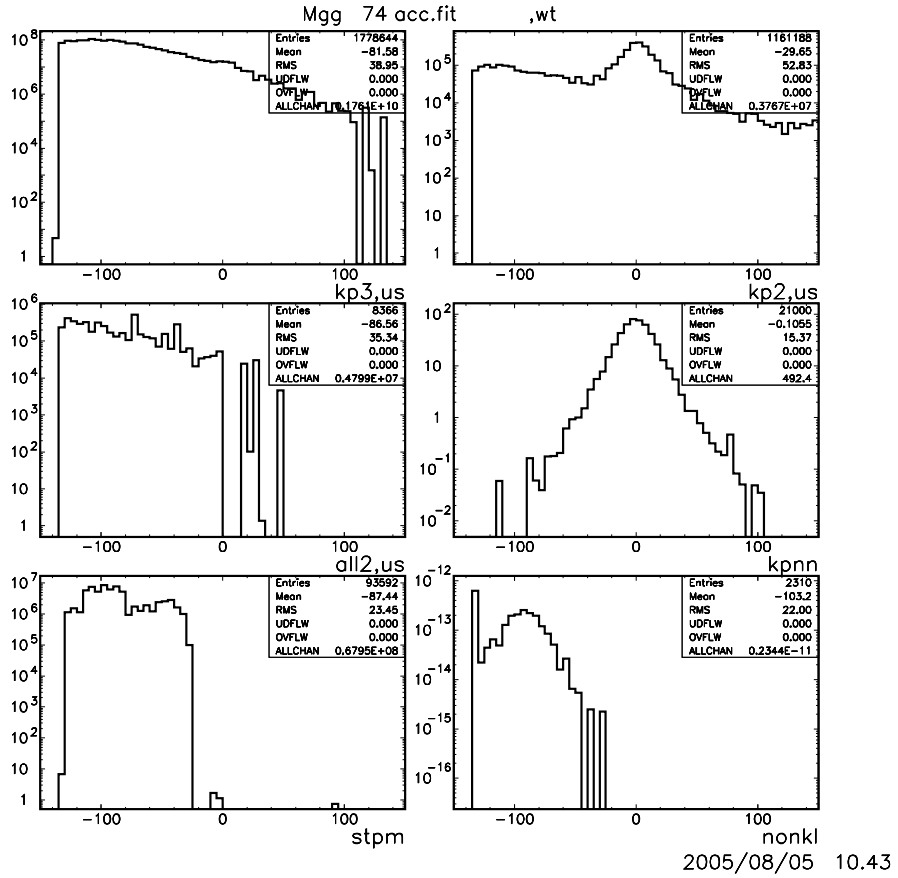


Figure 8: Distribution of Mgg for  $K_L^0 \rightarrow \pi^0 \pi^0 \pi^0$ ,  $K_L^0 \rightarrow \pi^0 \pi^0$ ,  $2K_L^0$ , signal, stopped muons &  $K_L^0$  and non- $K_L^0$  decays from top, left to right. The “GeomAcc” and “GoodFit” cuts have been applied to the upper six plots. The “GeomAcc”, “GoodFit” and “Fiducial” cuts have been applied to the lower size plots. The distributions are weighted.

2005/08/05 10.43

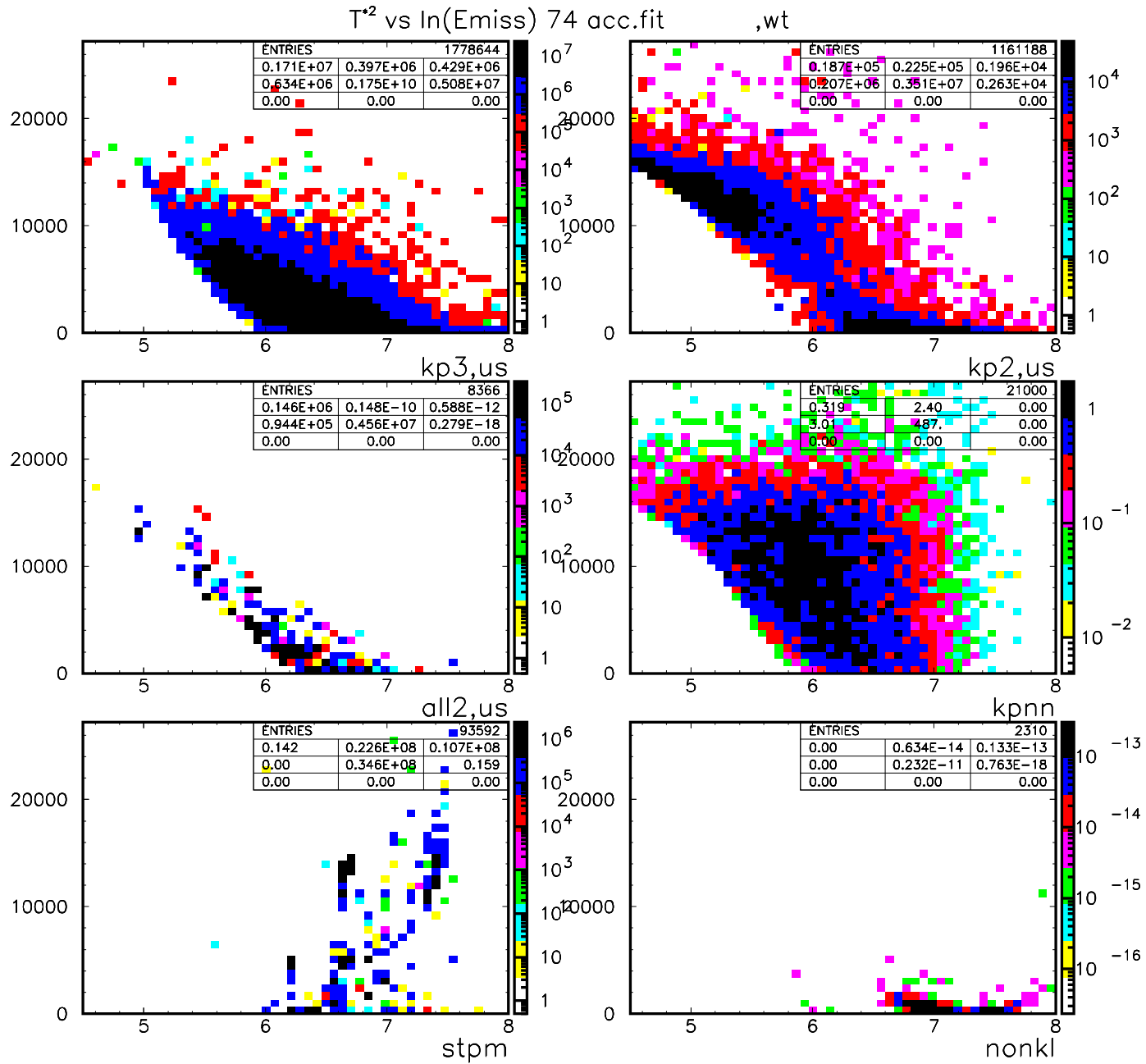


Figure 9: Distribution of  $T^{*2}$  vs  $\ln(E_{\text{miss}})$  for  $K_L^0 \rightarrow \pi^0 \pi^0 \pi^0$ ,  $K_L^0 \rightarrow \pi^0 \pi^0$ ,  $2K_L^0$ , signal, stopped muons &  $K_L^0$  and non- $K_L^0$  decays from top, left to right. The “GeomAcc” and “GoodFit” cuts have been applied. The distributions are weighted.

2005/08/05 10.43

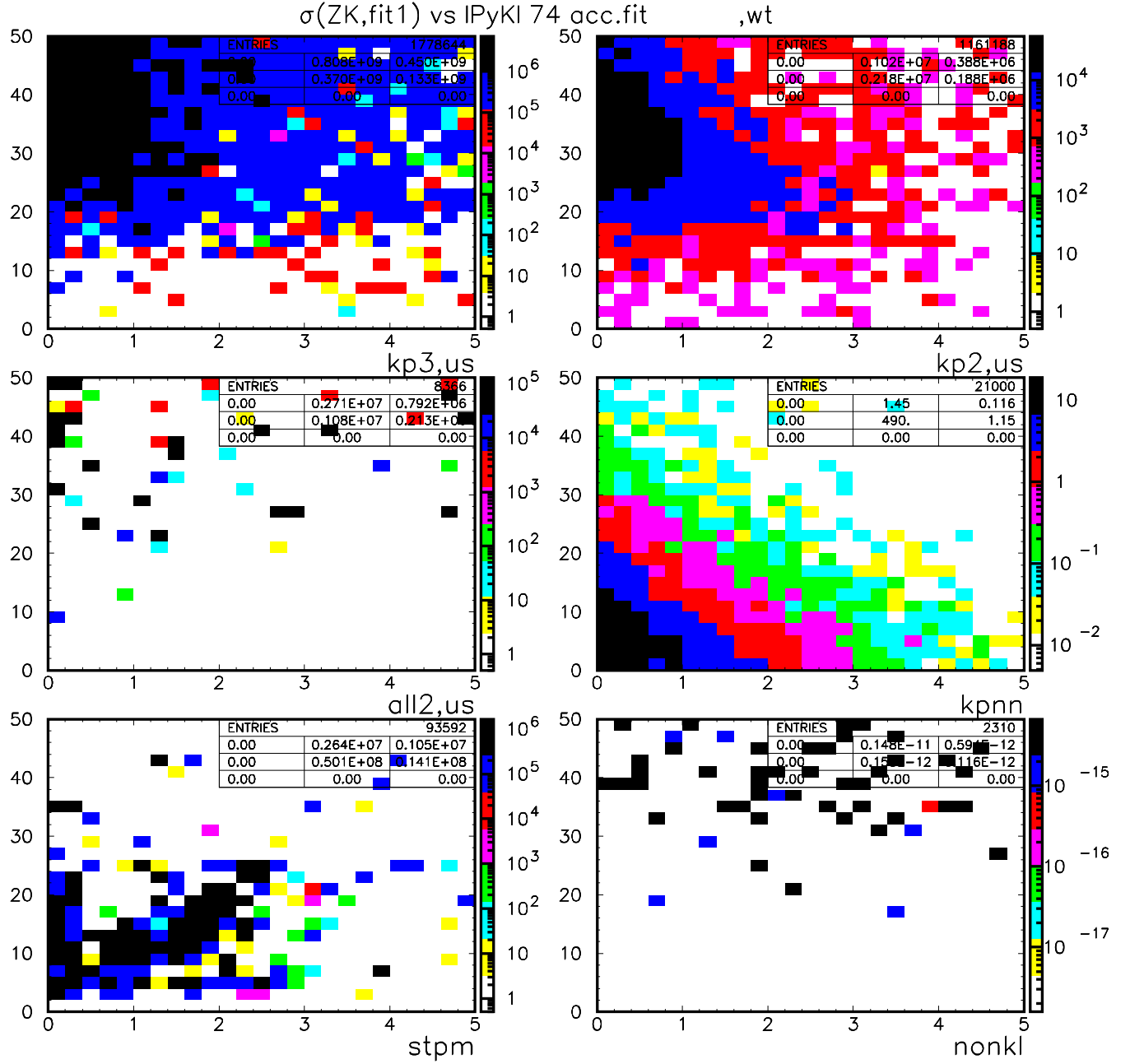


Figure 10: Distribution of  $\text{sgZK1}$  vs the y-component of the  $\text{K}_L^0$  momentum  $p_y(K)$  for  $\text{K}_L^0 \rightarrow \pi^0\pi^0\pi^0$ ,  $\text{K}_L^0 \rightarrow \pi^0\pi^0$ ,  $2\text{K}_L^0$ , signal, stopped muons &  $\text{K}_L^0$  and non- $\text{K}_L^0$  decays from top, left to right. The “GeomAcc” and “GoodFit” cuts have been applied. The distributions are weighted.

2005/08/05 10.43

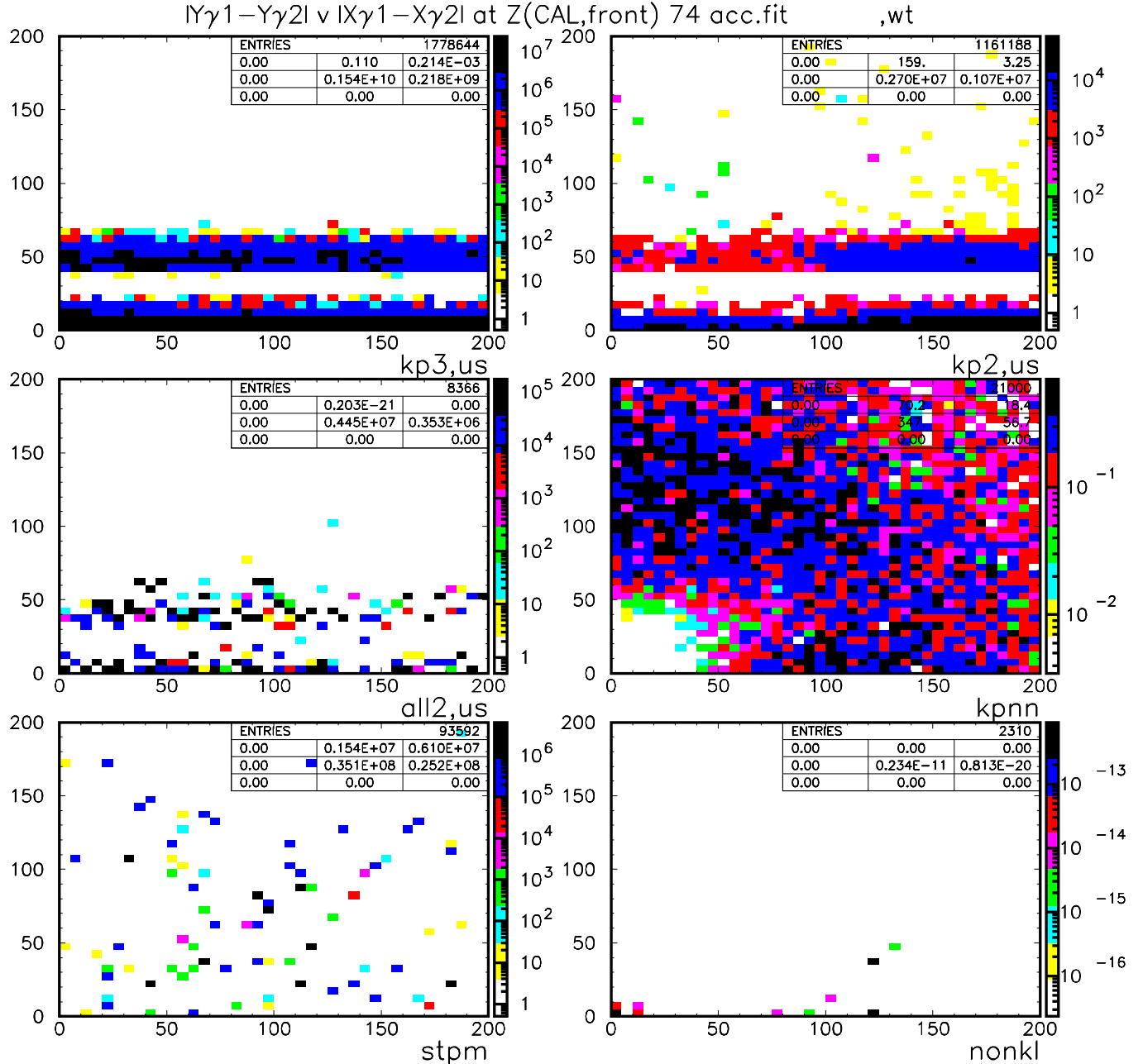


Figure 11: Distribution of  $|y_1 - y_2|$  vs  $|x_1 - x_2|$  where  $y_i$  is the projected  $x$  position of the  $i^{\text{th}}$  candidate photon projected to the  $z$  position of the upstream end of the calorimeter. for  $K_L^0 \rightarrow \pi^0 \pi^0 \pi^0$ ,  $K_L^0 \rightarrow \pi^0 \pi^0$ ,  $2K_L^0$ , signal, stopped muons &  $K_L^0$  and non- $K_L^0$  decays from top, left to right. The “GeomAcc” and “GoodFit” cuts have been applied. The distributions are weighted.

## 5 Expected background rates

The expected background rates with the loosest likelihood cut are shown in Tables 1 and 2 for the **stpm** and **nonkl** backgrounds, respectively. This is the same likelihood cut used to produce the results in TN137 [1]. The expected rates are based on the assumption that there are  $1.27 \times 10^{15}$  useful  $K_L^0$  exiting the spoiler in a 12000 hour run as in TN137 [1].

Both backgrounds are negligible based on these estimates. The most effective single cut at suppressing the **stpm** background is the cut in the  $E_g$  vs  $\chi_{2n}$  that is labelled  $E_g$  in Table 1. As noted earlier, further optimization of this cut is possible.

The **nonkl** background is completely suppressed by the **YatCL** cut that was designed to suppress background from  $K_L^0$  decays upstream of the decay region based on the detector geometry. Presumably the “Way upstream Veto” proposed in TN137 [1] could aid in suppressing the **nonkl** background.

Table 3 lists the efficiencies of selected cuts after the application of the “GeomAcc” cut for the **all2.us**, **nonkl** and **stpm** backgrounds and the signal. The purpose of this table is two-fold. It gives the efficiency of each cut after a setup cut (“GeomAcc”) and it allows comparison with an alternate analysis of the **all2.us** background [4]. Similar Tables 4, 5 and 6 list the efficiencies of selection cuts after successive application of the “GoodFit”, “Fiducial” and “MisRecon” cuts.

## 6 Summary and discussion and summary

Both the **stpm** and **nonkl** backgrounds can be brought under control with straightforward cuts. Ideally we would like to be able to estimate these backgrounds from the data.

To estimate the **stpm** background from the data we could identify stopped muons by following the  $\pi \rightarrow \mu \rightarrow e$  decay chain and then overlay these events onto either events with simulated  $K_L^0$  decays or real events acquired with a minimum bias (or appropriate) trigger. Such samples could be used both to design cuts to suppress the **stpm** background as well as measure the background.

It is not clear how to estimate the **nonkl** background from the data. One possible avenue would be to select events with either with a hit in the “Way upstream Veto” or failing the **YatCL** cut. For the background from  $K_L^0$  decays upstream of the decay region, these two cuts could be effective in a bifurcated analysis as used by E949 because  $K_L^0$  decays produce particles in addition to the photons that strike the PR and form  $\pi^0$  candidates. However, some fraction of the photons that comprise the **nonkl** background will not be accompanied by additional, detectable tracks.

Unweighted						Expected numbers of events						Cut	
N(pass)	Eff.1st	N(pass)	Eff.seq	Nbefore	Nafter	N(pass)	Eff.1st	N(pass)	Eff.seq	Nbefore	Nafter	Eff.last	
0.310E+10	0.00	0.310E+10	0.00	0.310E+10	0.310E+10	0.00	0.127E+16	0.00	0.127E+16	0.00	0.127E+16	0.00	NONE
0.220E+07	0.710E-03	0.220E+07	0.710E-03	12.0	12.0	1.00	0.431E+11	0.340E-04	0.431E+11	0.340E-04	0.833E-07	0.833E-07	Accpt
0.139E+08	0.44E-02	0.124E+07	0.563	12.0	12.0	1.00	0.717E+11	0.565E-04	0.205E+11	0.474	0.833E-07	0.833E-07	1.00
0.507E+07	0.163E-02	0.914E+06	0.738	12.0	12.0	1.00	0.866E+09	0.681E-06	0.222E+09	0.108E-01	0.833E-07	0.833E-07	1.00
0.442E+07	0.142E-02	0.468E+05	0.512E-01	12.0	12.0	1.00	0.469E+11	0.369E-04	0.679E+08	0.307	0.833E-07	0.833E-07	1.00
0.502E+07	0.162E-02	0.252E+05	0.538	15.0	12.0	0.800	0.298E+11	0.23E-04	0.375E+08	0.551	0.833E-07	0.833E-07	1.00
0.145E+08	0.466E-02	0.228E+05	0.907	12.0	12.0	1.00	0.396E+11	0.311E-04	0.159E+08	0.425	0.833E-07	0.833E-07	XK
0.947E+07	0.305E-02	0.114E+05	0.500	12.0	12.0	1.00	0.603E+11	0.47E-04	0.146E+08	0.919	0.833E-07	0.833E-07	1.00
0.624E+07	0.201E-02	0.724E+04	0.634	25.0	12.0	0.480	0.134E+11	0.105E-04	0.882E+05	0.604E-02	0.833E-07	0.833E-07	ZK
0.168E+08	0.541E-02	0.662E+04	0.914	14.0	12.0	0.857	0.115E+12	0.905E-04	19.5	0.221E-03	0.833E-07	0.833E-07	1.00
0.779E+07	0.251E-02	0.302E+04	0.455	12.0	12.0	1.00	0.369E+11	0.291E-04	17.8	0.915	0.833E-07	0.833E-07	1.00
0.452E+06	0.146E-03	519.	0.172	13.0	12.0	0.923	0.103E+10	0.811E-06	0.111	0.621E-02	0.833E-07	0.833E-07	1.00
0.168E+08	0.541E-02	519.	1.00	12.0	12.0	1.00	0.132E+12	0.10E-03	0.111	1.00	0.833E-07	0.833E-07	1.00
0.168E+08	0.541E-02	515.	0.992	12.0	12.0	1.00	0.601E+10	0.473E-05	0.111	1.000	0.833E-07	0.833E-07	1.00
0.126E+07	0.408E-03	250.	0.485	57.0	12.0	0.211	0.209E+11	0.165E-04	0.475E-05	0.430E-04	0.230E-06	0.833E-07	Eg
0.938E+07	0.303E-02	219.	0.876	12.0	12.0	1.00	0.196E+10	0.15E-05	0.351E-05	0.738	0.833E-07	0.833E-07	1.00
0.719E+07	0.232E-02	57.0	0.260	12.0	12.0	1.00	0.816E+10	0.642E-05	0.145E-06	0.412E-01	0.833E-07	0.833E-07	Mgg
0.168E+08	0.541E-02	57.0	1.00	12.0	12.0	1.00	0.132E+12	0.10E-03	0.145E-06	1.00	0.833E-07	0.833E-07	E*pi
0.767E+06	0.24E-03	12.0	0.211	57.0	12.0	0.211	0.729E+08	0.57E-07	0.833E-07	0.576	0.145E-06	0.833E-07	0.576
													Like

Table 1: Cut survival table for **stpm** background. The seven columns on the left are unweighted events. The next seven columns are weighted by decay probability,  $K_L^0$  production rate, conversion probability and veto inefficiency to produce the expected number of events for the full running period of KOPIO. The fifteenth column lists the five letter acronym of the applied cuts defined in TN137 [1]. The top row (Cut “NONE”) gives the total number of simulated events. The first column is the number of events that pass the cut. The second column is the efficiency of the cut when it is applied first, before all other cuts. The third column is the number of events passing the cuts listed in the sequence in the fifteenth column. The fourth column is the efficiency of the cut when applied in sequence. The fifth column is the number of events passing all other cuts except the cut in that row. The sixth column is the number of events passing all cuts. The seventh column is the efficiency of the cut when applied last, after all other cuts. Columns eight through fourteen are similar.

Unweighted						Expected numbers of events						Cut	
N(pass)	Eff.1st	N(pass)	Eff.seq	Nbefore	Nafter	N(pass)	Eff.1st	N(pass)	Eff.seq	Nbefore	Nafter	Eff.last	
0.201E+10	0.00	0.201E+10	0.00	0.201E+10	0.201E+10	0.00	0.127E+16	0.00	0.127E+16	0.00	0.127E+16	0.00	NONE
0.443E+05	0.220E-04	0.443E+05	0.220E-04	0.00	0.00	0.00	0.809E+09	0.636E-06	0.809E+09	0.636E-06	0.00	0.00	Accpt
0.548E+07	0.272E-02	0.829E+04	0.187	0.00	0.00	0.00	0.175E+12	0.138E-03	0.239E+09	0.295	0.00	0.00	Ierr
0.775E+06	0.386E-03	0.761E+04	0.918	0.00	0.00	0.00	0.129E+11	0.101E-04	0.233E+09	0.976	0.00	0.00	ValKL
0.168E+08	0.835E-02	0.750E+04	0.985	0.00	0.00	0.00	0.537E+12	0.423E-03	0.228E+09	0.980	0.00	0.00	Chi2n
0.168E+08	0.835E-02	0.733E+04	0.978	0.00	0.00	0.00	0.636E+12	0.501E-03	0.227E+09	0.996	0.00	0.00	delT
0.168E+08	0.835E-02	0.721E+04	0.983	0.00	0.00	0.00	0.632E+12	0.497E-03	0.223E+09	0.981	0.00	0.00	XK
0.137E+08	0.681E-02	0.427E+04	0.593	0.00	0.00	0.00	0.440E+12	0.347E-03	0.118E+09	0.527	0.00	0.00	Yk
0.598E+07	0.297E-02	0.424E+04	0.993	0.00	0.00	0.00	0.148E+12	0.116E-03	0.117E+09	0.995	0.00	0.00	ZK
0.00	0.00	0.00	0.00	0.00	0.00	0.00	0.00	0.00	0.00	0.00	0.00	0.00	YatCL
0.168E+08	0.835E-02	0.00	0.00	0.00	0.00	0.00	0.628E+12	0.497E-03	0.00	0.00	0.00	0.00	DOCA
0.479E+07	0.238E-02	0.00	0.00	0.00	0.00	0.00	0.138E+12	0.108E-03	0.00	0.00	0.00	0.00	DK12
0.168E+08	0.835E-02	0.00	0.00	0.00	0.00	0.00	0.633E+12	0.498E-03	0.00	0.00	0.00	0.00	sgZK1
0.336E+07	0.167E-02	0.00	0.00	0.00	0.00	0.00	0.637E+11	0.502E-04	0.00	0.00	0.00	0.00	PK
0.668E+07	0.332E-02	0.00	0.00	0.00	0.00	0.00	0.209E+12	0.165E-03	0.00	0.00	0.00	0.00	Eg
0.316E+07	0.157E-02	0.00	0.00	0.00	0.00	0.00	0.626E+11	0.493E-04	0.00	0.00	0.00	0.00	Mnu2
0.807E+05	0.402E-04	0.00	0.00	0.00	0.00	0.00	0.201E+08	0.159E-07	0.00	0.00	0.00	0.00	Mgg
0.168E+08	0.835E-02	0.00	0.00	0.00	0.00	0.00	0.637E+12	0.501E-03	0.00	0.00	0.00	0.00	E*pi
0.222E+05	0.110E-04	0.00	0.00	0.00	0.00	0.00	0.733E+06	0.577E-09	0.00	0.00	0.00	0.00	Like

Table 2: Cut survival table for **nonkl** background. The seven columns on the left are unweighted events. The next seven columns are weighted by conversion probability and veto inefficiency to produce the expected number of events for the full running period of KOPIO. The fifteenth column lists the five letter acronym of the applied cuts defined in TN137 [1]. The top row (Cut “NONE”) gives the total number of simulated events. The first column is the number of events that pass the cut. The second column is the efficiency of the cut when it is applied first, before all other cuts. The third column is the number of events passing the cuts listed in the sequence in the fifteenth column. The fourth column is the efficiency of the cut when applied in sequence. The fifth column is the number of events passing all other cuts except the cut in that row. The sixth column is the number of events passing all cuts. The seventh column is the efficiency of the cut when applied last, after all other cuts. Columns eight through fourteen are similar.

<b>all2.us</b>				<b>nonkl</b>				Classes or cuts	
Unweighted		Expected Nevts		Unweighted		Expected Nevts			
N(pass)	Eff	N(weight)	Eff.wt	N(pass)	Eff	N(weight)	Eff.wt		
0.140E+10	0.00	0.127E+16	0.00	0.201E+10	0.00	0.127E+16	0.00	NONE GeomAcc	
0.947E+04	0.676E-05	0.115E+08	0.904E-08	0.443E+05	0.220E-04	0.809E+09	0.636E-06		
0.890E+04	0.939	0.105E+08	0.918	0.410E+05	0.926	0.692E+09	0.856	XK	
0.443E+04	0.468	0.631E+07	0.549	0.579E+04	0.131	0.134E+09	0.166	Yk	
0.690E+04	0.729	0.744E+07	0.648	0.191E+05	0.430	0.335E+09	0.414	ZK	
0.108E+04	0.114	0.899E+06	0.783E-01	5.00	0.113E-03	0.206E+06	0.255E-03	Mgg	
0.914E+04	0.965	0.109E+08	0.948	0.435E+05	0.982	0.802E+09	0.992	E*pi	
0.918E+04	0.969	0.110E+08	0.958	0.365E+05	0.825	0.769E+09	0.951	PK	
0.444E+04	0.469	0.392E+07	0.341	0.344E+05	0.776	0.699E+09	0.864	Mnu2	
0.947E+04	1.00	0.115E+08	1.00	0.443E+05	1.00	0.809E+09	1.00	Emiss	
212.	0.224E-01	0.145E+06	0.126E-01	1.00	0.226E-04	0.592E+05	0.732E-04	Like	
<b>stpm</b>				<b>kpnn</b>				Classes or cuts	
Unweighted		Expected Nevts		Unweighted		Expected Nevts			
N(pass)	Eff	N(weight)	Eff.wt	N(pass)	Eff	N(weight)	Eff.wt		
0.310E+10	0.00	0.127E+16	0.00	0.500E+05	0.00	0.381E+05	0.00	NONE GeomAcc	
0.220E+07	0.710E-03	0.431E+11	0.340E-04	0.105E+05	0.210	493.	0.129E-01		
0.168E+07	0.763	0.109E+11	0.252	0.104E+05	0.990	488.	0.989	XK	
0.422E+06	0.192	0.169E+11	0.392	0.102E+05	0.973	480.	0.974	Yk	
0.521E+06	0.237	0.501E+10	0.116	0.728E+04	0.693	347.	0.704	ZK	
0.256E+06	0.116	0.148E+09	0.343E-02	0.101E+05	0.957	473.	0.960	Mgg	
0.215E+07	0.977	0.431E+11	0.998	0.104E+05	0.994	490.	0.994	E*pi	
0.170E+07	0.773	0.205E+10	0.476E-01	0.103E+05	0.980	480.	0.974	PK	
0.752E+06	0.342	0.648E+09	0.150E-01	0.799E+04	0.760	358.	0.726	Mnu2	
0.220E+07	1.00	0.431E+11	1.00	0.105E+05	1.00	493.	1.00	Emiss	
0.271E+05	0.123E-01	0.927E+07	0.215E-03	0.740E+04	0.704	335.	0.679	Like	

Table 3: Individual cut efficiencies after application of the “GeomAcc” cuts for the **all2.us**, **nonkl** and **stpm** backgrounds and signal for the same likelihood cut used for the other tables and figures in this note. For each background there are four columns. The first column contains the number of events that pass the cut after application of the “GeomAcc” cut. The second column is the efficiency of the cut after application of the “GeomAcc” cut. The third and fourth column are the similar to the first two, excepted that the events are weighted.

<b>all2.us</b>				<b>nonkl</b>				Classes or cuts	
Unweighted		Expected Nevts		Unweighted		Expected Nevts			
N(pass)	Eff	N(weight)	Eff.wt	N(pass)	Eff	N(weight)	Eff.wt		
0.140E+10	0.00	0.127E+16	0.00	0.201E+10	0.00	0.127E+16	0.00	NONE GeomAcc.GoodFit	
0.418E+04	0.299E-05	0.480E+07	0.378E-08	0.750E+04	0.373E-05	0.228E+09	0.180E-06		
0.406E+04	0.971	0.465E+07	0.970	0.738E+04	0.984	0.224E+09	0.982	XK	
0.228E+04	0.546	0.272E+07	0.566	0.443E+04	0.591	0.119E+09	0.520	Yk	
0.311E+04	0.743	0.318E+07	0.663	0.569E+04	0.759	0.168E+09	0.735	ZK	
496.	0.119	0.302E+06	0.630E-01	4.00	0.533E-03	0.206E+06	0.903E-03	Mgg	
0.410E+04	0.981	0.465E+07	0.970	0.688E+04	0.918	0.226E+09	0.990	E*pi	
0.418E+04	1.000	0.480E+07	1.00	0.748E+04	0.997	0.228E+09	0.998	PK	
0.277E+04	0.663	0.225E+07	0.469	0.746E+04	0.995	0.228E+09	0.997	Mnu2	
0.418E+04	1.00	0.480E+07	1.00	0.750E+04	1.00	0.228E+09	1.00	Emiss	
143.	0.342E-01	0.731E+05	0.152E-01	1.00	0.133E-03	0.592E+05	0.259E-03	Like	
<b>stpm</b>				<b>kpnn</b>				Classes or cuts	
Unweighted		Expected Nevts		Unweighted		Expected Nevts			
N(pass)	Eff	N(weight)	Eff.wt	N(pass)	Eff	N(weight)	Eff.wt		
0.310E+10	0.00	0.127E+16	0.00	0.500E+05	0.00	0.381E+05	0.00	NONE GeomAcc.GoodFit	
0.468E+05	0.151E-04	0.679E+08	0.535E-07	0.105E+05	0.210	492.	0.129E-01		
0.425E+05	0.909	0.386E+08	0.567	0.104E+05	0.990	487.	0.989	XK	
0.245E+05	0.525	0.525E+08	0.772	0.102E+05	0.974	480.	0.975	Yk	
0.258E+05	0.551	0.187E+07	0.275E-01	0.728E+04	0.693	347.	0.704	ZK	
0.218E+04	0.466E-01	0.101E+06	0.148E-02	0.101E+05	0.958	473.	0.961	Mgg	
0.413E+05	0.882	0.346E+08	0.509	0.104E+05	0.994	490.	0.994	E*pi	
0.466E+05	0.996	0.676E+08	0.995	0.103E+05	0.980	479.	0.974	PK	
0.431E+05	0.921	0.650E+08	0.957	0.798E+04	0.760	357.	0.726	Mnu2	
0.468E+05	1.00	0.679E+08	1.00	0.105E+05	1.00	492.	1.00	Emiss	
710.	0.152E-01	3.84	0.565E-07	0.740E+04	0.704	334.	0.679	Like	

Table 4: Individual cut efficiencies after application of the “GeomAcc” and “GoodFit” cuts for the **all2.us**, **nonkl** and **stpm** backgrounds and signal for the same likelihood cut used for the other tables and figures in this note. For each background there are four columns. The first column contains the number of events that pass the cut after application of the “GeomAcc” and “GoodFit” cuts. The second column is the efficiency of the cut after application of the “GeomAcc” and “GoodFit” cuts. The third and fourth column are the similar to the first two, excepted that the events are weighted.

all2.us				nonkl				Classes or cuts
Unweighted		Expected Nevts		Unweighted		Expected Nevts		
N(pass)	Eff	N(weight)	Eff.wt	N(pass)	Eff	N(weight)	Eff.wt	
0.140E+10	0.00	0.127E+16	0.00	0.201E+10	0.00	0.127E+16	0.00	NONE
160.	0.11E-06	21.0	0.165E-13	0.00	0.00	0.00	0.00	GeomAcc.GoodFit.Fiducial
15.0	0.938E-01	0.139E-04	0.661E-06	0.00	0.00	0.00	0.00	Mgg
160.	1.00	21.0	1.00	0.00	0.00	0.00	0.00	E*pi
160.	1.00	21.0	1.00	0.00	0.00	0.00	0.00	PK
94.0	0.587	18.4	0.875	0.00	0.00	0.00	0.00	Mnu2
160.	1.00	21.0	1.00	0.00	0.00	0.00	0.00	Emiss
5.00	0.312E-01	0.31E-12	0.151E-13	0.00	0.00	0.00	0.00	Like
stpm				kpnn				Classes or cuts
Unweighted		Expected Nevts		Unweighted		Expected Nevts		
N(pass)	Eff	N(weight)	Eff.wt	N(pass)	Eff	N(weight)	Eff.wt	
0.310E+10	0.00	0.127E+16	0.00	0.500E+05	0.00	0.381E+05	0.00	NONE
0.662E+04	0.21E-05	19.5	0.153E-13	0.624E+04	0.125	305.	0.800E-02	GeomAcc.GoodFit.Fiducial
451.	0.681E-01	1.12	0.575E-01	0.602E+04	0.966	295.	0.967	Mgg
0.643E+04	0.971	18.6	0.955	0.621E+04	0.996	304.	0.997	E*pi
0.659E+04	0.994	19.5	1.00	0.613E+04	0.983	298.	0.978	PK
0.603E+04	0.910	19.5	1.000	0.471E+04	0.755	217.	0.712	Mnu2
0.662E+04	1.00	19.5	1.00	0.624E+04	1.00	305.	1.00	Emiss
143.	0.216E-01	1.12	0.575E-01	0.442E+04	0.709	205.	0.673	Like

Table 5: Individual cut efficiencies after application of the “GeomAcc”, “GoodFit” and “Fiducial” cuts for the **all2.us**, **nonkl** and **stpm** backgrounds and signal for the same likelihood cut used for the other tables and figures in this note. For each background there are four columns. The first column contains the number of events that pass the cut after application of the “GeomAcc”, “GoodFit” and “Fiducial” cuts. The second column is the efficiency of the cut after application of the “GeomAcc”, “GoodFit” and “Fiducial” cuts. The third and fourth column are the similar to the first two, excepted that the events are weighted.

<b>all2.us</b>				<b>nonkl</b>				Classes or cuts	
Unweighted		Expected Nevts		Unweighted		Expected Nevts			
N(pass)	Eff	N(weight)	Eff.wt	N(pass)	Eff	N(weight)	Eff.wt		
0.140E+10	0.00	0.127E+16	0.00	0.201E+10	0.00	0.127E+16	0.00	NONE	
3.00	0.21E-08	0.315E-12	0.248E-27	0.00	0.00	0.00	0.00	GeomAcc.GoodFit.Fiducial.MisRecon	
3.00	1.00	0.315E-12	1.00	0.00	0.00	0.00	0.00	Mgg	
3.00	1.00	0.315E-12	1.00	0.00	0.00	0.00	0.00	E*pi	
3.00	1.00	0.315E-12	1.00	0.00	0.00	0.00	0.00	PK	
3.00	1.00	0.315E-12	1.00	0.00	0.00	0.00	0.00	Mnu2	
3.00	1.00	0.315E-12	1.00	0.00	0.00	0.00	0.00	Emiss	
1.00	0.333	0.315E-12	0.999	0.00	0.00	0.00	0.00	Like	
<b>stpm</b>				<b>kpnn</b>				Classes or cuts	
Unweighted		Expected Nevts		Unweighted		Expected Nevts			
N(pass)	Eff	N(weight)	Eff.wt	N(pass)	Eff	N(weight)	Eff.wt		
0.310E+10	0.00	0.127E+16	0.00	0.500E+05	0.00	0.381E+05	0.00	NONE	
519.	0.167-06	0.111	0.870E-16	0.564E+04	0.113	277.	0.725E-02	GeomAcc.GoodFit.Fiducial.MisRecon	
197.	0.380	0.736E-05	0.666E-04	0.558E+04	0.988	273.	0.989	Mgg	
517.	0.996	0.111	1.00	0.563E+04	0.997	276.	0.998	E*pi	
515.	0.992	0.111	1.000	0.555E+04	0.983	271.	0.978	PK	
446.	0.859	0.111	1.000	0.432E+04	0.765	200.	0.722	Mnu2	
519.	1.00	0.111	1.00	0.564E+04	1.00	277.	1.00	Emiss	
57.0	0.110	0.230E-06	0.208E-05	0.414E+04	0.734	193.	0.697	Like	

Table 6: Individual cut efficiencies after application of the “GeomAcc”, “GoodFit”, “Fiducial” and “MisRecon” cuts for the **all2.us**, **nonkl** and **stpm** backgrounds and signal for the same likelihood cut used for the other tables and figures in this note. For each background there are four columns. The first column contains the number of events that pass the cut after application of the “GeomAcc”, “GoodFit”, “Fiducial” and “MisRecon” cuts. The second column is the efficiency of the cut after application of the “GeomAcc”, “GoodFit”, “Fiducial” and “MisRecon” cuts. The third and fourth column are the similar to the first two, excepted that the events are weighted.

## 7 Acknowledgements

I thank Andrei Poblagev for many useful discussions and for producing the sample of events used for the **nonkl** studies. I thank Marvin Blecher for producing the sample of stopped muons. I thank the National Science Board of the National Science Foundation for having the wisdom and foresight to approve RSVP.

## References

- [1] D.E. Jaffe, *Background from  $K_L^0$  decays upstream of the decay region*, KOPIO TN137, 16 June 05.
- [2] D.E. Jaffe, *FastMC User Manual*, KOPIO TN089, 20 Oct 2004.
- [3] D.E. Jaffe, *Neutrons and the vacuum upstream of the decay region*, KOPIO TN138, 14 July 05.
- [4] Carol Scarlett, *Background from 2 random  $K_L^0 \rightarrow 2\gamma$ 's in the Pre-Radiator*, in preparation.